PROCEEDINGS, 51st Workshop on Geothermal Reservoir Engineering
Stanford University, Stanford, California, February 9-11, 2026
SGP-TR-230

Predicting Fracture Intensity and Aperture with Physics-Informed Machine Learning for Utah FORGE

Khomchan Promneewat[1], Zhi Ye[1], and Ahmad Ghassemi[2]

1. South Dakota School of Mines and Technology

2. The University of Oklahoma

zhi.ye@sdsmt.edu

Keywords: Fracture Intensity (P32), Fracture Aperture, Machine Learning, Geothermal Wells, Utah FORGE

ABSTRACT

This study applies supervised machine learning using Extreme Gradient Boosting (XGBoost) with physics-informed formulations to predict fracture intensity (P_{32}) and fracture aperture in deep geothermal reservoirs using drilling and logging-while-drilling data from the Utah FORGE project. To reduce reliance on costly image logs and enable real-time, ahead-of-bit fracture characterization, we apply a depth-based machine learning (ML) prediction strategy that trains the model on shallow-depth data and predicts fracture properties across the remaining well interval. This approach relies on extrapolative, rather than interpolative, predictions and therefore involves a trade-off between prediction accuracy and logging requirements compared to traditional machine learning approaches that depend on full-length wellbore logs. Model performance is evaluated against conventional machine learning approaches, including baseline models without physics-informed formulations, and further compared under scenarios with and without physics-informed features, as well as with or without reduced feature sets. Results show that training the model on approximately 50-60% of the shallow well interval is sufficient to achieve reliable ahead-of-bit predictions of fracture intensity and aperture. Additionally, wavelet-based feature transformations enhance predictive accuracy, and the inclusion of physics-informed formulations further improves performance, particularly in predicting fracture intensity.

1. INTRODUCTION

Fracture intensity and fracture aperture are key parameters in reservoir evaluation because of their direct relationship to reservoir permeability (Zhang et al., 2023). In geothermal energy production, particularly in Enhanced Geothermal Systems (EGS), maintaining permeability is necessary for sustaining continuous fluid circulation between injection and production wells (Kaya et al., 2011). Fracture intensity and aperture are two of the main parameters in the fractured reservoir stimulation, pressure optimization, and long-term reservoir performance.

Fracture characterization along the wellbore is commonly performed using borehole image logs, such as the Formation Microresistivity Imaging (FMI) logs, which provide high-resolution images for measuring fracture aperture and estimating fracture intensity. Although the FMI log provides a high accuracy compared to core-based methods, the application is constrained by high operational costs, computational demands, and temperature limitations (SLB, 2025). In high-temperature geothermal environments, FMI tools often cannot be deployed at greater depths, creating data gaps between drilling operations and fracture interpretation, particularly where well cooling is impractical or risky (Kaldal et al., 2015; Sánchez-Pastor et al., 2021).

Previous studies have investigated fracture intensity prediction using statistical, geomechanical, and machine learning approaches (de Oliveira Neto et al., 2025; Feng et al., 2018; Gao et al., 2023; Ifrene et al., 2023). However, many of these machine learning models rely on depth as a key input feature and report a strong correlation between depth and fracture intensity (Azadivash et al., 2024). These are mostly effective in shallow reservoirs, this dependence on depth limits application in deep-well projects, where fracture data are sparse, and logging tools such as FMI are restricted by high temperatures, particularly in geothermal environments.

To respond to these limitations, this study proposes a machine learning framework for predicting fracture intensity in deep wells using only drilling and logging-while-drilling data, without relying on depth as a predictive feature. Machine learning (ML) analysis is applied on a well-by-well basis, as deep-well projects generally involve significantly fewer wells compared to shallow reservoirs. The approach evaluates traditional machine learning (ML) alongside depth-based prediction strategies, in which both full and reduced feature sets are examined. This study extends the workflow from Promneewat et al. (2025), by applying physics-informed methods derived from drilling efficiency to improve model performance. The methodology is validated using data from two vertical and one inclined well in the Utah FORGE project, to develop more reliable fracture intensity and aperture prediction tools for geothermal and related subsurface applications.

2. BACKGROUND

2.1 Fracture Intensity

Fracture intensity can be evaluated at different spatial scales (Table 1). In a one-dimensional framework (P_{11}), fracture is defined as the frequency of fractures per unit length along a borehole. When in two dimensions (P_{21} and P_{22}), fracture intensity corresponds to the total

fracture length normalized by the borehole surface area. In three dimensions (P_{31}, P_{32}, and P_{33}), fractures are quantified by the fracture surface area or volume per unit volume of the rock mass. Among these parameters, P_{32} is widely used in subsurface engineering and has been adopted in practice, as demonstrated by numerous studies.

Table 1. Fracture intensity in spatial dimensions (modified from Dershowitz and Herda (1992)).

Measurement Region Dimension / Dimension of Fracture Measure	1D: Line Measurement (e.g., Borehole or Scanline)	2D: Area Measurement (e.g., Trace Plane)	3D: Volume Measurement (e.g., Rock Mass)
	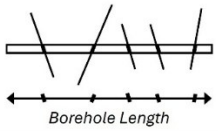	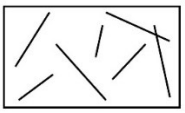	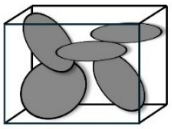
Number of Fractures	**P_{11}**: Number of fractures per unit length along a borehole or scanline (inverse spacing) [L^{-1}]	**P_{21}**: Number of fractures per unit area of a trace plane [L^{-2}]	**P_{31}**: Number of fractures per unit volume of rock [L^{-3}]
One Dimension Less than Measurement Region		**P_{22}**: Total length of fracture traces per unit area of the trace plane [L^{-1}]	**P_{32}**: Total area of fractures per unit volume of rock [L^{-1}]
Same Dimension as Measurement Region			**P_{33}**: Total volume of fractures per unit volume of rock [-]

2.2 Supervised Machine Learning

Supervised machine learning trains models on labeled data to capture the relationship between input features and known outputs. Extreme Gradient Boosting (XGBoost) is used to predict fracture intensity and aperture, as well as to provide insight into the influence of input features.

2.2.1 Extreme Gradient Boosting (XGBoost)

This method is based on decision trees and improves performance by iteratively correcting errors from previous trees. Model learning is tracked using an objective function, where decreasing or stable values indicate effective learning, while increasing values may signal overfitting (Chen et al., 2015). The objective function combines the loss function with a regularization term. Model optimization uses the Mean Squared Error loss function, computed by comparing successive iterations through a second-order Taylor expansion (Eq. 1 and 2). The regularization term stabilizes model learning by constraining the objective function and reducing the risk of overfitting.

$$loss\ function\ (MSE) = \frac{1}{n}\sum_{i=1}^{n}(y_i - \hat{y}_i)^2 \tag{1}$$

where n is the number of samples, y_i is the actual value, and $\hat{y}_i$ is the predicted value.

$$\hat{y}_i^{(t)} = \hat{y}_i^{(t-1)} + \eta \cdot -\left[\frac{\sum g_i}{\sum h_i + \lambda}\right] \tag{2}$$

where $\hat{y}_i^{(t)}$ is the predicted value at iteration t, $\hat{y}_i^{(t-1)}$ is the value from the previous iteration, η is the learning rate, g_i is the gradient (first derivative), h_i is the Hessians (second derivative), and λ represents the regularization term.

2.2.2 Physic-informed input

To incorporate physical understanding into the machine learning framework, physics-informed formulations are applied. These formulations generally enhance predictive performance, particularly by improving the magnitude of predictions when relevant physical features are included in the model. In this study, Penetration Efficiency per applied load (PEP) (Eq. 3) and Normalized Penetration Efficiency (NPE) (Eq. 4) were used to capture the mechanical response of the rock to drilling forces. These features involve domain-based knowledge in the data-driven models, enhancing the magnitude prediction when these features are involved in classification.

$$Penetration\ Efficiency\ per\ applied\ load\ (PEP) = \frac{Rate\ of\ Penetration\ (ROP)}{Applied\ Load\ (WOB)} \tag{3}$$

$$Normalized\ Penetration\ Efficiency\ (NPE) = \frac{Rate\ of\ Penetration\ (ROP)}{Applied\ Load\ (WOB) + Round\ per\ minutes\ (RPM)} \quad (4)$$

Drilling efficiency derived from the rate of penetration and applied load is sensitive to formation strength and damage boundary state. Highly fractured formations (expect high P_{32}) tend to break easily, leading to increased penetration efficiency (Teale, 1965). Accordingly, high Penetration Efficiency per applied load (PEP) and Normalized Penetration Efficiency (NPE) are physically consistent with elevated P_{32} and are used here as indirect indicators of fracture intensity in the machine learning models.

2.3 Study Area: Utah FORGE

The Utah Frontier Observatory for Research in Geothermal Energy (FORGE) is a U.S. Department of Energy-funded field laboratory focused on developing Enhanced Geothermal Systems for clean energy production. The site includes eight vertical and inclined wells with a total length of nearly 10 miles. Geologically, the FORGE site is dominated by plutonic granitic rock, with shallow sedimentary and volcaniclastic units overlying the pluton on the western side (Moore et al., 2020). This study uses data from wells 56-32, 78B-32, and 16B(78)-32.

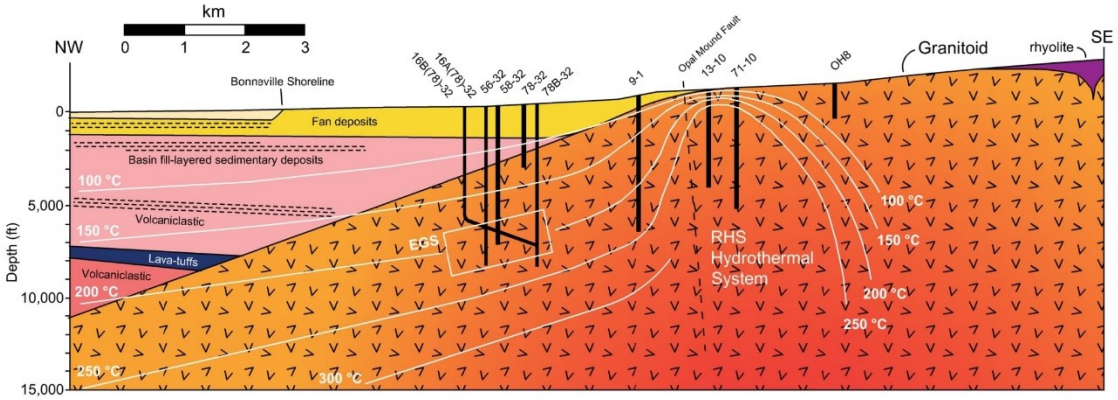

Figure 1. Overview cross-section of the Utah FORGE project, showing an unconformity between a massive granitoid formation and beds of volcaniclastic and basin sedimentary deposits, along with some project wellbores (modified from Moore et al. (2020)).

2.4 Dataset and Method Approach

2.4.1 Dataset

Data from wells 56-32, 78B-32, and 16B(78)-32 include drilling and logging-while-drilling parameters at selected depths, such as hook load, rate of penetration, mud return flow rate, RPM, weight on bit, P-wave, S-wave, gamma ray, Poisson ratio, Sonic Porosity, Penetration Efficiency per applied load (PEP), Normalized Penetration Efficiency (NPE), aperture, and fracture intensity (P_{32}) (Figure 2). Each feature is statistically processed prior to model training to enhance the machine learning algorithms to capture dynamic variations in the feature (Figure 3).

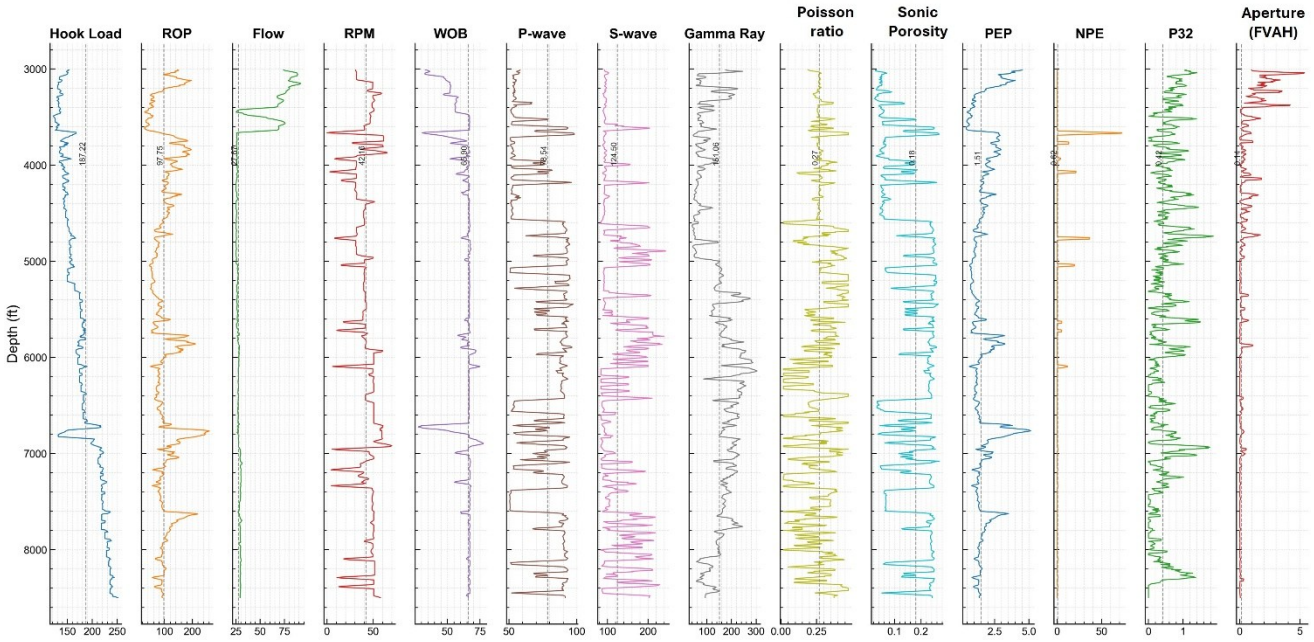

Figure 2. Example of data from well 78B-32. Each column represents a drilling and logging feature.

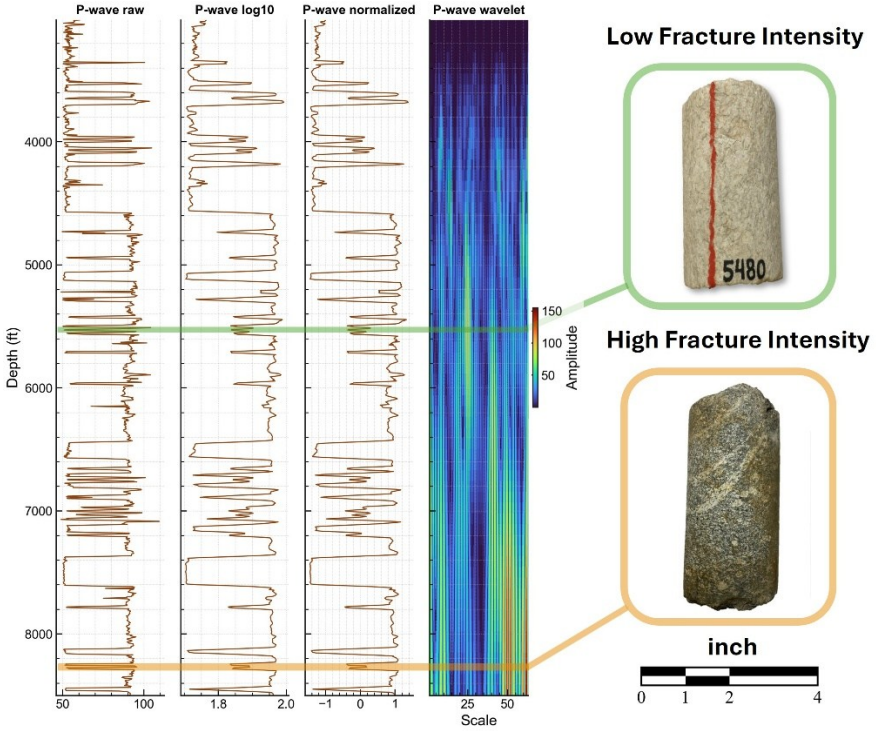

Figure 3. P-wave features along well 78B-32 under different statistical representations, including raw, log-transformed, normalized, and wavelet domains. The figure also shows core samples from low- and high-fracture zones, illustrating that feature transform can enhance the capture of the target feature change.

2.4.2 Method Approach

This study divides the training, validation, and testing strategies into three main methods. Scenario 1 represents a traditional machine learning approach, in which data are randomly split along the well without considering depth. Scenario 2 applies a depth-based prediction strategy using the full feature set, with training, validation, and testing ordered from the shallow to the deepest sections of the wellbore. Scenario 3 uses a depth-based prediction strategy with a reduced feature set, incorporating only half of the most influential features identified in Scenario 2 (Figure 4).

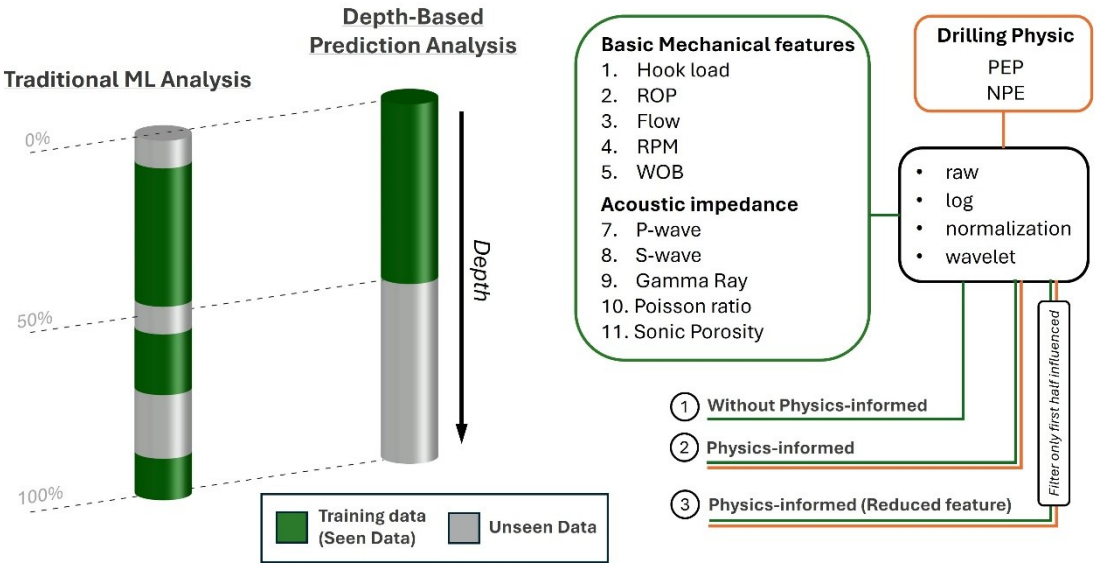

Figure 4. Training and testing strategies for each scenario. In the traditional machine learning approach, data from the entire wellbore are available to the model, providing a complete overview of fracture intensity and aperture. In contrast, the depth-based prediction strategy restricts the model to data up to the end of the training interval, represented by the green shaded area.

3. RESULTS

The analysis was performed using multiple training, validation, and testing splits (20/40/40, 30/35/35, 40/30/30, 50/25/25, 60/20/20, 70/15/15, and 80/10/10). The setting 60/20/20 is selected to represent an example of comparison between the prediction and actual fracture intensity and aperture. Feature importance was extracted for each well trajectory and then averaged across all splits. The results are divided into the following sections:

3.1 Traditional Analysis Prediction Performance

The model prediction performance of the traditional analysis models for fracture intensity (P_{32}) and fracture aperture (FVAH) across different training, validation, and testing split ratios is summarized in Table 2. For P_{32}, consistently high performance is observed across all split configurations, with test R^2 values ranging from 0.84 to 0.89 and RMSE values between 0.17 and 0.20. When incorporating physics-informed, the model achieves slightly higher performance, with consistent improvements in most split cases. In contrast, the reduced physics-informed performance is lower compared to the full physics-informed model. For FVAH, model performance shows improvement in direct response to the split configuration change, with test R^2 values increasing from approximately 0.54 at lower training fractions to over 0.74 at higher training fractions. Differences between models with and without physics-informed for FVAH remain small across all splits, trend to smaller, and the reduced feature model maintains performance comparable to the full feature set.

Table 2. Performance of the traditional analysis model for P_{32} and fracture aperture (FVAH) across training, validation, and testing splits.

		20/40/40		30/35/35		40/30/30		50/25/25		60/20/20		70/15/15		80/10/10	
		R^2	RMSE	R^2	RMSE	R^2	RMSE	R^2	RMSE	R^2	RMSE	R^2	RMSE	R^2	RMSE
P32	Without Physic-informed	0.850	0.188	0.849	0.192	0.841	0.200	0.857	0.184	0.871	0.177	0.876	0.179	0.891	0.168
	Physics-informed	0.854	0.186	0.853	0.190	0.847	0.197	0.861	0.182	0.881	0.170	0.876	0.178	0.889	0.169
	Physic-informed (reduced feature)	0.854	0.186	0.851	0.191	0.845	0.198	0.856	0.185	0.879	0.171	0.874	0.180	0.887	0.171
FVAH	Without Physic-informed	0.540	0.417	0.613	0.351	0.680	0.290	0.684	0.290	0.658	0.310	0.668	0.315	0.738	0.220
	Physics-informed	0.524	0.425	0.604	0.354	0.669	0.295	0.683	0.291	0.657	0.310	0.656	0.321	0.742	0.217
	Physic-informed (reduced feature)	0.524	0.425	0.600	0.356	0.666	0.296	0.679	0.292	0.653	0.312	0.669	0.314	0.741	0.218

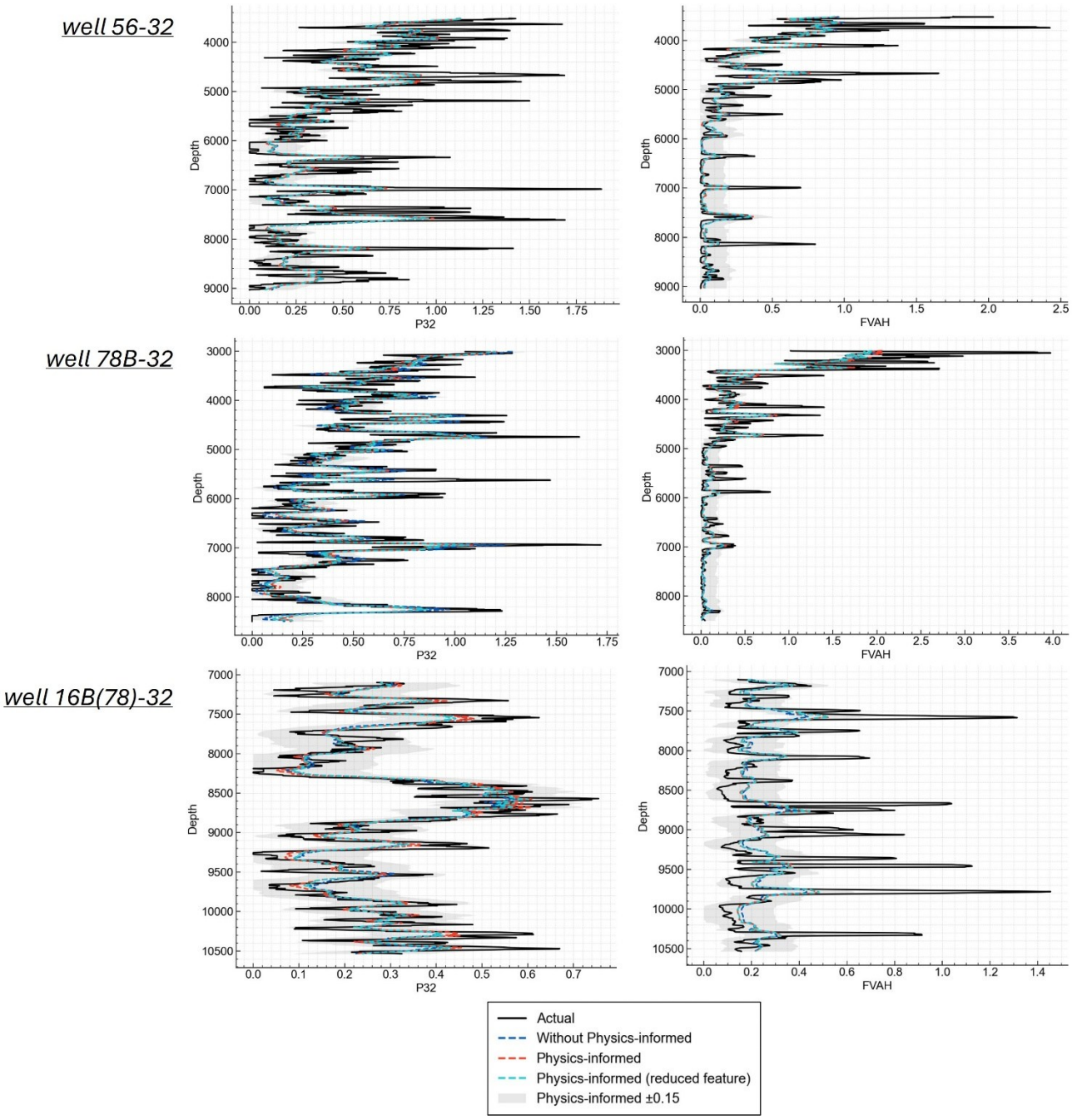

Figure 5. Comparison of actual fracture intensity (P_{32}) and fracture aperture (FVAH) with predictions from traditional machine learning models, including models without physics-informed features, with physics-informed features, and with reduced physics-informed features.

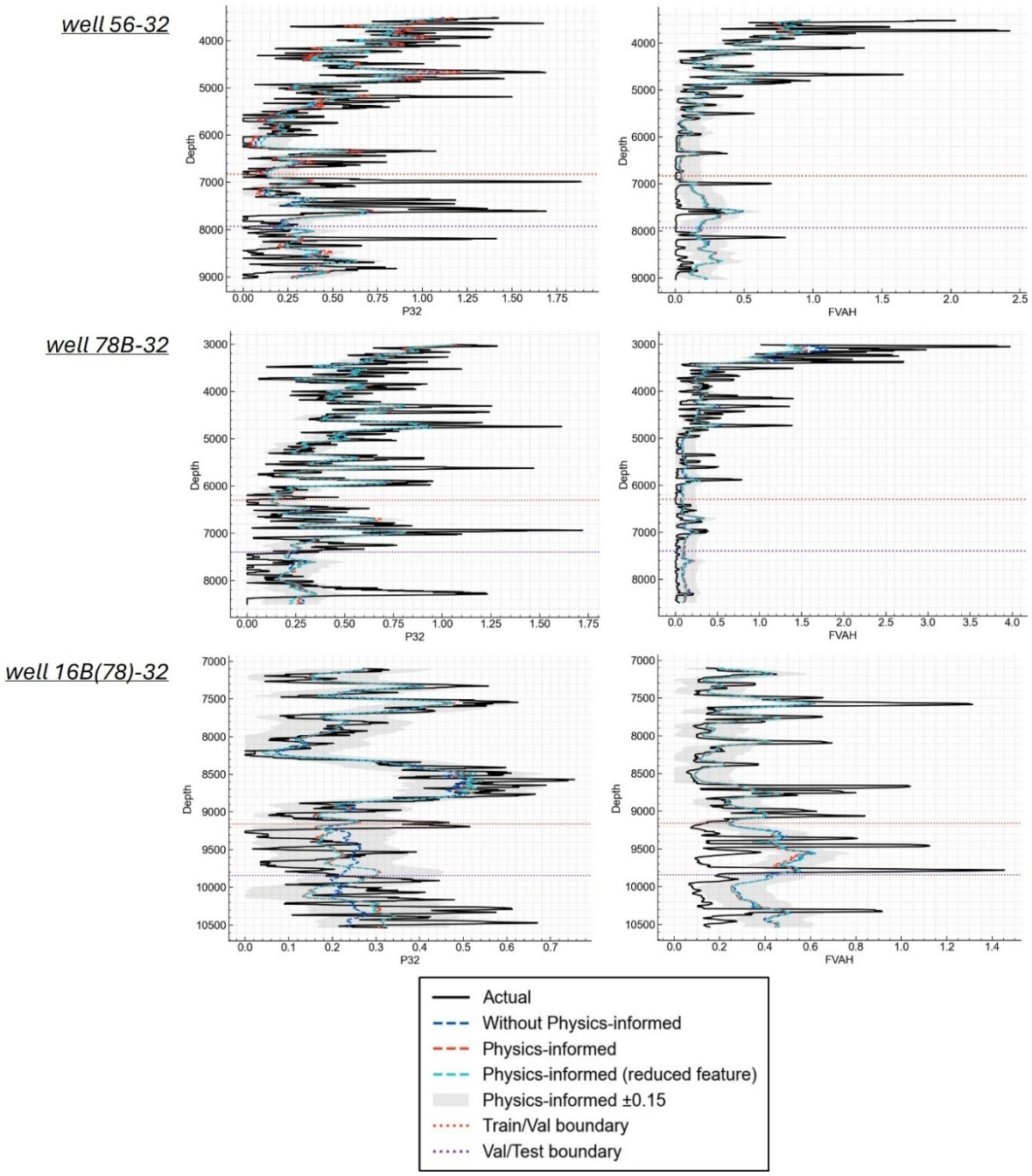

Figure 6. Comparison of actual fracture intensity (P_{32}) and fracture aperture (FVAH) with predictions from depth-based analysis models, including models without physics-informed features, with physics-informed, and with reduced-featured physics-informed.

3.2 Depth-based Analysis Prediction Performance

The depth-based analysis model performance for fracture intensity (P32) and fracture aperture (FVAH) across different training, validation, and testing split ratios is summarized in Table 3. For P32, moderate predictive performance is observed across all split configurations, with test R^2 values increasing from approximately 0.61 at lower training fractions to a maximum of about 0.71 at the 50/25/25 split, followed by a slight decline at higher training fractions. Corresponding RMSE values decrease as training data increases up to the 50/25/25 split and then increase slightly for larger training fractions. Models with and without physics-informed show comparable performance across all splits, and the reduced-featured physics-informed shows similar results. For FVAH, model performance is more variable, with negative or near-zero test R^2 values at lower training fractions (20/40/40 and 30/35/35), transitioning to positive R^2 values as the training fraction increases. The highest FVAH test performance is observed for training fractions between 50% and 70%, with test R^2 values reaching approximately 0.57 and corresponding RMSE values decreasing to around 0.14-0.16. Differences between physics-informed, reduced-feature, and non–physics-informed models remain small across all split configurations.

Table 3. Performance of the depth-based analysis model for P32 and fracture aperture (FVAH) across training, validation, and testing splits.

		20/40/40		30/35/35		40/30/30		50/25/25		60/20/20		70/15/15		80/10/10	
		R^2	RMSE	R^2	RMSE	R^2	RMSE	R^2	RMSE	R^2	RMSE	R^2	RMSE	R^2	RMSE
P32	Without Physic-informed	0.611	0.285	0.640	0.268	0.660	0.266	0.706	0.203	0.670	0.221	0.637	0.234	0.645	0.249
	Physics-informed	0.624	0.280	0.637	0.270	0.660	0.266	0.700	0.205	0.686	0.216	0.631	0.237	0.637	0.252
	Physic-informed (reduced feature)	0.617	0.283	0.637	0.270	0.664	0.265	0.698	0.206	0.679	0.218	0.655	0.229	0.637	0.252
FVAH	Without Physic-informed	-0.382	0.266	-0.265	0.261	0.463	0.167	0.530	0.157	0.515	0.145	0.571	0.141	0.557	0.169
	Physics-informed	-0.398	0.266	-0.093	0.250	0.452	0.169	0.527	0.158	0.521	0.144	0.568	0.142	0.561	0.167
	Physic-informed (reduced feature)	-0.375	0.266	-0.105	0.253	0.463	0.167	0.531	0.157	0.517	0.145	0.565	0.142	0.565	0.167

3.2 Feature Importance

Table 4 presents the feature importance rankings for vertical and inclined wells. Across both well orientations, transformed features rank higher than original raw data, with wavelet and normalized forms showing more frequently among higher-ranked predictors, while logarithmic transforms tend to appear at lower ranks. In vertical wells, acoustic impedance features show the highest rankings, with wavelet-transformed S-wave and P-wave velocities ranked first and second, followed by mechanical features such as RPM and hook load. In inclined wells, mechanical drilling parameters dominate the highest ranks, with wavelet-transformed ROP, RPM, hook load, mud flow, and WOB representing the top positions, while acoustic features are ranked at intermediate levels. Gamma ray features show at mid-level ranks in both well types, whereas Poisson ratio and sonic porosity features consistently rank in the lower half of the feature set.

Table 4. Feature importance rankings for each well trajectory. Vertical wells include Wells 56-32 and 78B-32, and the inclined well corresponds to Well 16B(78)-32. Lower ranking values indicate higher feature importance, and green shading highlights features with relatively stronger contributions to the prediction model.

			Vertical well	Inclined well
Mechanical features	Hook load	raw	8	8
		log	22	40
		norm	16	13
		wavelet	4	3
	ROP	raw	33	6
		log	39	29
		norm	35	11
		wavelet	25	1
	Mud flow	raw	11	9
		log	23	32
		norm	17	14
		wavelet	9	4
	RPM	raw	7	7
		log	21	30
		norm	15	12
		wavelet	3	2
	WOB	raw	34	10
		log	40	33
		norm	36	15
		wavelet	26	5
Acoustic Impedance features	P-wave	raw	6	19
		log	20	35
		norm	14	23
		wavelet	2	16
	S-wave	raw	5	21
		log	19	36
		norm	13	24
		wavelet	1	18
	Gamma Ray	raw	12	20
		log	24	34
		norm	18	22
		wavelet	10	17

	Poisson ratio	raw	28	28
		log	32	40
		norm	30	38
		wavelet	26	26
	Sonic Porosity	raw	27	27
		log	31	39
		norm	29	37
		wavelet	25	25

4. DISCUSSIONS

4.1 Model Comparison

4.1.1 Traditional ML Analysis and Depth-based Prediction Analysis

A comparison between the traditional machine learning (ML) analysis and the depth-based prediction analysis represents clear differences in prediction performance for fracture intensity (P32) and fracture aperture (FVAH). Traditional ML models show consistently high and stable test performance across all training, validation, and testing split configurations. In contrast, depth-based prediction models exhibit lower and more variable performance, particularly for FVAH, with test R^2 values improving as the training fraction increases. For P32, depth-based models achieve moderate test performance, with the highest values observed at intermediate training fractions.

Although the traditional ML analysis demonstrates higher prediction performance in terms of evaluation metrics, the approach does not respond to the objective of reducing downhole operation length (Figure 7). Traditional ML approaches require full-length FMI logging to generate predictions along the entire wellbore, whereas the depth-based prediction analysis requires only a certain proportion of data from shallow depths to train the model and predict fracture properties for the remaining wellbore. Based on the results, using approximately 50-60% of the well depth for training provides sufficient predictive performance for subsequent depth prediction. This approach is more practical for field applications, as it can significantly reduce FMI logging length, operational time, and associated risks, which directly translate to cost savings, particularly in high-temperature geothermal drilling environments.

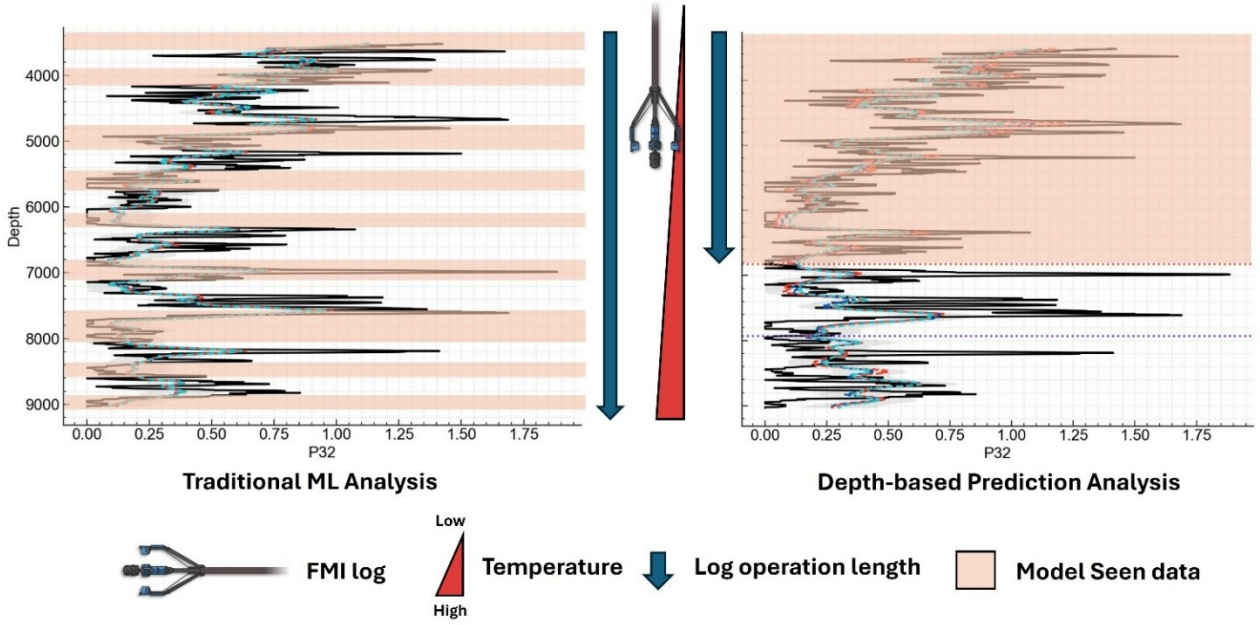

Figure 7. Illustration of the different FMI logging lengths required for the traditional machine learning analysis and the depth-based prediction analysis. The logging length determines the amount of data available to the prediction model for training (seen data) and therefore influences model performance. Shorter FMI logging lengths are associated with lower downhole temperatures and shorter operation times.

4.1.2 Physic-informed enhance prediction model performance

Across both traditional and depth-based analyses, models incorporating physics-informed generally achieve improved prediction performance compared to models without physics-informed inputs, particularly for fracture intensity (P_{32}). In the traditional analysis, physics-informed models consistently show slightly higher test R^2 values and lower RMSE across most split configurations, while reduced-feature physics-informed models perform comparably to the full feature set. In contrast, improvements for fracture aperture (FVAH) are limited, with only minor differences observed between physics-informed and non–physics-informed models, indicating that physics-informed drilling efficiency metrics are more closely related to fracture density than to fracture opening.

4.2 Scale Effects in Fracture Intensity and Aperture Prediction

Different collected spatial fundamentals explain why fracture intensity (P_{32}) can be more effectively predicted using mechanical, acoustic impedance, and physics-informed methods compared with fracture aperture (FVAH). P_{32} is defined as the median per one-foot interval of total fracture surface area per unit volume and therefore represents an aggregated, bulk-scale property that integrates fracture behavior over a larger depth or spatial interval. As a result, P_{32} exhibits smoother variability with moving depth and stronger correlations with drilling-response and energy-based features. In contrast, fracture aperture is defined as the median aperture within each one-foot interval, representing a highly localized property that is sensitive to small-scale geological and mechanical variations. This local scale leads to abrupt spatial changes and more inconsistent relationships with drilling and acoustic parameters, which are typically measured at coarser or integrated scales. These scale differences explain why prediction models consistently achieve better performance for fracture intensity than for fracture aperture, and why aperture prediction remains more sensitive to training data coverage and feature selection.

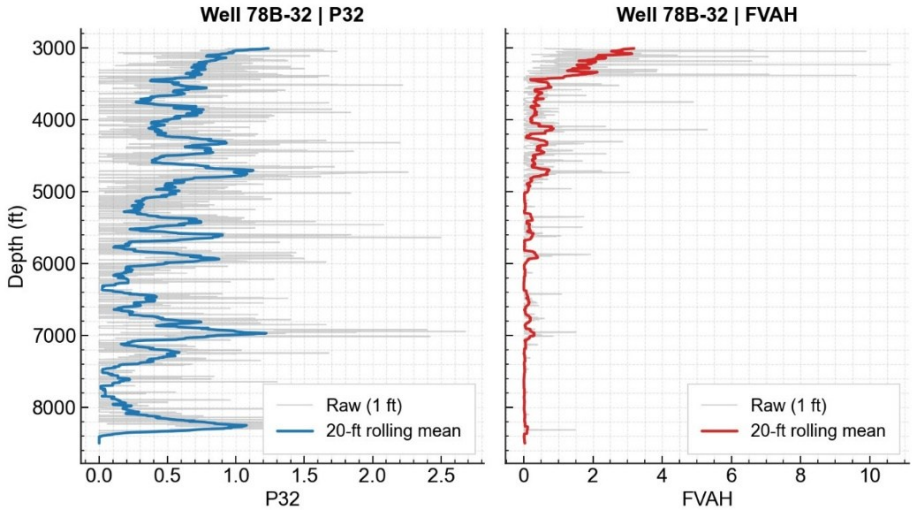

Figure 9. Comparison of raw (1-ft interval) and 20-ft rolling-mean profiles of P32 and FVAH in Well 78B-32. The rolling-mean profiles display the greater spatial distribution of fracture intensity compared with the less dynamic aperture signal changing, indicating that a limited training length interval may be insufficient to capture the full variability of fracture aperture.

4.3 Physical Drivers of Feature Importance

The feature importance patterns represent the interplay between measurement scale, tool geometry, and the physical processes governing drilling and logging responses. Wavelet-transformed features contribute strongly to the predictions because wavelet representations capture signal variability across multiple spatial scales and interval windows, allowing the model to respond to both localized fluctuations and broader depth-dependent trends. Rather than relying on mechanical drilling features, the physics-informed formulation embeds mechanical and energy-related constraints directly into the learning process, enabling the model to better represent fracture-related responses using existing drilling and logging inputs. In vertical wells, acoustic impedance features tend to be more influential due to the near-perpendicular orientation of logging tools relative to the formation, which enhances sensitivity to elastic property contrasts. In inclined wells, geometric effects associated with the deviated well trajectory reduce the effectiveness of acoustic measurements, and the physics-informed formulation makes mechanical drilling parameters dominant in the prediction model (Figure 10).

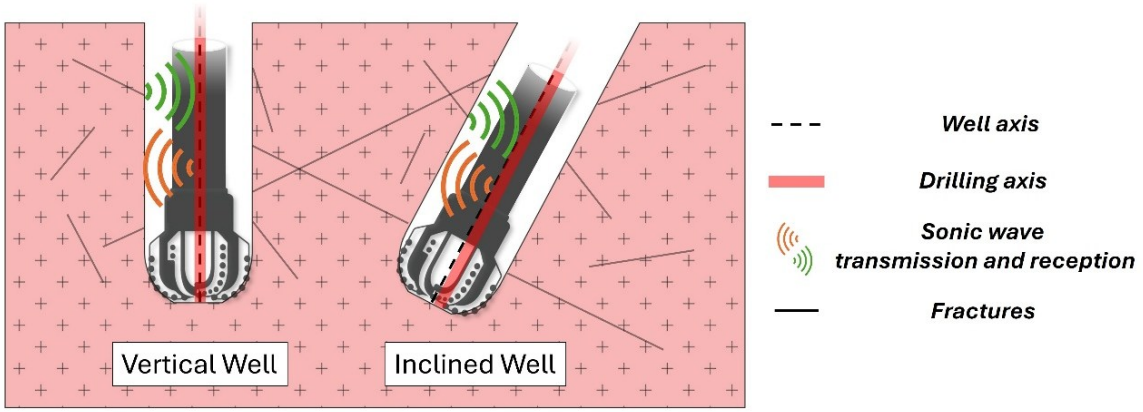

Figure 10. Conceptual illustration comparing sonic wave transmission and reception in vertical and inclined wells. In vertical wells, the near-perpendicular orientation of the logging tools relative to the drilling axis enhances the sensitivity of acoustic impedance measurements to elastic contrasts. In inclined wells, the nature of the deviated drilling axis generates geometric

limitations that reduce the effectiveness of acoustic measurements, leading mechanical drilling parameters to dominate in capturing fracture-related responses.

5. CONCLUSION

The results demonstrate a clear trade-off between prediction accuracy and operational efficiency in fracture characterization. Traditional machine learning analyses achieve consistently higher and more stable prediction performance for both fracture intensity (P_{32}) and fracture aperture (FVAH) because the models are trained using full-length wellbore data. However, this approach requires complete FMI logging coverage and therefore does not reduce the downhole operation length. In contrast, the depth-based prediction strategy provides a practical alternative by using only partial shallow-depth data for model training. The results indicate that using approximately 50-60% of the well depth is sufficient to achieve acceptable predictive performance for the remaining interval, practically reducing logging length, operational time, and downhole risk. This reduction links to cost and safety advantages, particularly in high-temperature geothermal environments where logging operations are constrained.

The incorporation of physics-informed formulations further improves model performance, particularly for fracture intensity prediction. Instead of using only mechanical drilling features, the physics-informed approach incorporates mechanical and energy-related constraints directly into the learning framework, enhance model to capture fracture-related. Performance improvements are greater for fracture intensity (P_{32}) than for fracture aperture (FVAH), representing a scale effect in fracture characterization. Fracture intensity represents a bulk property that integrates fracture behavior over a larger spatial interval, leading to smoother variations along the wellbore and stronger relationships with drilling and logging. In contrast, fracture aperture is a highly localized property with limited spatial continuity, making more difficult to predict accurately using limited training data.

Feature importance results show that transformed representations, particularly wavelet-based features, effectively capture multiscale patterns relevant to fracture prediction. Feature contributions vary with well trajectory, with acoustic impedance measurements being more influential in vertical wells and mechanical drilling responses contributing more strongly in the inclined wells. Overall, combining depth-based prediction strategies with physics-informed formulations provides a reliable and practical framework for predicting fracture intensity and aperture in deep geothermal wells.

ACKNOWLEDGMENT

We gratefully acknowledge support from the South Dakota Board of Regents Competitive Research Grant and collaboration with the University of Oklahoma. The data used in this study were obtained from the Utah FORGE database within the Geothermal Data Repository.

REFERENCES

Azadivash, A., Soleymani, H., Seifirad, A., Sandani, A., Yahyaee, F., & Kadkhodaie, A. (2024). Robust fracture intensity estimation from petrophysical logs and mud loss data: A multi-level ensemble modeling approach. *Journal of Petroleum Exploration and Production Technology*, *14*(7), 1859-1878.

Chen, T., He, T., Benesty, M., Khotilovich, V., Tang, Y., Cho, H., Chen, K., Mitchell, R., Cano, I., & Zhou, T. (2015). Xgboost: extreme gradient boosting. *R package version 0.4-2*, *1*(4), 1-4.

de Oliveira Neto, E. R., Fernandes, F. J. D., Fatah, T. Y. A., Dias, R. M., da Piedade, Z. R. T., Freire, A. F. M., & Lupinacci, W. M. (2025). A data-driven approach to predict fracture intensity using machine learning for presalt carbonate reservoirs: A feasibility study in the Mero Field, Santos Basin, Brazil. *Energy Geoscience*, *6*(2), 100404.

Dershowitz, W. S., & Herda, H. H. (1992). Interpretation of fracture spacing and intensity. ARMA US rock mechanics/geomechanics symposium,

Feng, J., Li, L., Jin, J., Dai, J., & Luo, P. (2018). An improved geomechanical model for the prediction of fracture generation and distribution in brittle reservoirs. *PloS one*, *13*(11), e0205958.

Gao, G., Hazbeh, O., Davoodi, S., Tabasi, S., Rajabi, M., Ghorbani, H., Radwan, A. E., Csaba, M., & Mosavi, A. H. (2023). Prediction of fracture density in a gas reservoir using robust computational approaches. *Frontiers in Earth Science*, *10*, 1023578.

Ifrene, G., Irofti, D., Ni, R., Egenhoff, S., & Pothana, P. (2023). New insights into fracture porosity estimations using machine learning and advanced logging tools. *Fuels*, *4*(3), 333-353.

Kaldal, G. S., Jonsson, M. T., Palsson, H., & Karlsdottir, S. N. (2015). Structural modeling of the casings in high temperature geothermal wells. *Geothermics*, *55*, 126-137.

Kaya, E., Zarrouk, S. J., & O'Sullivan, M. J. (2011). Reinjection in geothermal fields: A review of worldwide experience. *Renewable and sustainable energy reviews*, *15*(1), 47-68.

Moore, J., McLennan, J., Pankow, K., Simmons, S., Podgorney, R., Wannamaker, P., Jones, C., Rickard, W., & Xing, P. (2020). The Utah Frontier Observatory for Research in Geothermal Energy (FORGE): a laboratory for characterizing, creating and sustaining enhanced geothermal systems. Proceedings of the 45th workshop on geothermal reservoir engineering,

Promneewat, K., Ye, Z., & Ghassemi, A. (2025). Machine Learning-Based Prediction of Fracture Characteristics from Drilling Data in Geothermal Wells. GRC Transactions, Reno, NV.

Sánchez-Pastor, P., Obermann, A., Reinsch, T., Ágústsdóttir, T., Gunnarsson, G., Tómasdóttir, S., Hjörleifsdóttir, V., Hersir, G., Ágústsson, K., & Wiemer, S. (2021). Imaging high-temperature geothermal reservoirs with ambient seismic noise tomography, a case study of the Hengill geothermal field, SW Iceland. *Geothermics*, *96*, 102207.

SLB. (2025). *FMI Fullbore formation Microimager. Well Logging | SLB.* Retrieved July 18 from https://www.slb.com/products-and-services/innovating-in-oil-and-gas/reservoir-characterization/surface-and-downhole-logging/wireline-openhole-logging/fmi-fullbore-formation-microimager#related-information

Teale, R. (1965). The concept of specific energy in rock drilling. *International Journal of Rock Mechanics and Mining Sciences & Geomechanics Abstracts*, *2*(1), 57-73. https://doi.org/10.1016/0148-9062(65)90022-7

Zhang, B., Wang, L., & Liu, J. (2023). Effect of Fracture Geometry Parameters on the Permeability of a Random Three-Dimensional Fracture Network. *Processes*, *11*(8). https://doi.org/10.3390/pr11082237